
Universiteit
Leiden
The Netherlands

A new type 2 copper cysteinate azurin: Involvement of an engineered exposed cysteine in copper binding trough internal rearrangement

Amsterdam, I.M.C. van; Ubbink, M.; Bosch, M. van den; Rotsaert, F.; Sander-Loehr, J.; Canters, G.W.

Citation
Amsterdam, I. M. C. van, Ubbink, M., Bosch, M. van den, Rotsaert, F., Sander-Loehr, J., & Canters, G. W. (2002). A new type 2 copper cysteinate azurin: Involvement of an engineered exposed cysteine in copper binding trough internal rearrangement. *The Journal Of Biological Chemistry, 277*(46), 44121-44130. doi:10.1074/jbc.M202977200

Version:	Publisher's Version
License:	Creative Commons CC BY 4.0 license
Downloaded from:	https://hdl.handle.net/1887/3608233

Note: To cite this publication please use the final published version (if applicable).

THE JOURNAL OF BIOLOGICAL CHEMISTRY
Vol. 277, No. 46, Issue of November 15, pp. 44121–44130, 2002
Printed in U.S.A.
© 2002 by The American Society for Biochemistry and Molecular Biology, Inc.

A New Type 2 Copper Cysteinate Azurin

INVOLVEMENT OF AN ENGINEERED EXPOSED CYSTEINE IN COPPER BINDING THROUGH INTERNAL REARRANGEMENT*

Received for publication, March 27, 2002, and in revised form, July 15, 2002
Published, JBC Papers in Press, August 16, 2002, DOI 10.1074/jbc.M202977200

Irene M. C. van Amsterdam‡, Marcellus Ubbink‡, Marieke van den Bosch‡, Frederik Rotsaert§, Joann Sanders-Loehr§, and Gerard W. Canters‡¶

From the ‡Leiden Institute of Chemistry, Gorlaeus Laboratories, University of Leiden, Einsteinweg 55, P. O. Box 9502, 2300 RA Leiden, The Netherlands and the §Department of Biochemistry and Molecular Biology, Oregon Graduate Institute of Science and Technology, Beaverton, Oregon 97006-8921

The double mutant H117G/N42C azurin exhibits tetragonal type 2 copper site characteristics with Cys^{42} as one of the copper ligands as concluded from spectroscopic evidence (UV-visible, EPR, and resonance Raman). Analysis of the kinetics of copper uptake by the apoprotein by means of stopped flow spectroscopy suggests that the solvent-exposed Cys^{42} assists in binding the metal ion and carrying it over to the active site where it becomes coordinated by, among others, a second cysteine, Cys^{112}. A structure is proposed in which the loop from residue 36 to 47 has rearranged to form a tetragonal type 2 copper site with Cys^{42} as one of the ligands. The process of copper uptake as observed for the double mutant may be relevant for a better understanding of the way copper chaperones accept and transfer metal ions in the living cell.

In an attempt to construct dimers of the electron transfer protein azurin from *Pseudomonas aeruginosa*, the double mutant H117G/N42C was constructed. The properties of this azurin variant in its monomeric form turned out to be quite unexpected and are the subject of the present paper. Experiments on the dimers that have been constructed from it will be described elsewhere.

Azurin from *P. aeruginosa* is a small blue copper protein that contains a type 1 copper site. Type 1 copper sites are characterized by an intense absorption band near 600 nm (ϵ = 3,000–6,000 M^{-1} cm^{-1}) and by EPR spectra with unusually small $A_\parallel$ values ($A_\parallel < 70 \times 10^{-4}$ cm^{-1}) (1). The copper ion in azurin is coordinated by three strong ligands (S^γ of Cys^{112} and N^δ of His^{117} and His^{46}) forming a trigonal plane around the copper and two weak axial ligands (S^δ of Met^{121} and backbone oxygen of Gly^{45}) (2, 3). Much has been learned about coordination geometry in cupredoxins by removal and replacement of copper ligands. An example is the replacement of His^{117} by glycine in azurin. The H117G mutation creates a gap in the protein surface through which the copper-containing active center becomes accessible for external ligands (4–6). Type 1 character is maintained when monodentate ligands such as imidazole and pyridine (derivatives), halides or azide are added. The site reverts to type 2 character when bidentate ligands such as histidine and histamine are added.

The introduction of an additional cysteine at position 42 produces a double mutant with unusual spectroscopic and mechanistic properties. We demonstrate in this work that the protein framework of the doubly mutated protein can undergo a major rearrangement leading to a metal site in which Cys^{42} acts as one of the copper ligands. This site has a unique spectroscopic fingerprint. Moreover, when the copper site is reconstituted by incubating the apoprotein with Cu(II), the Cys^{42} functions as an arm that catches the metal ion and carries it over to the active site where it becomes coordinated by, among others, a second cysteine, Cys^{112}. This process may be relevant for a better understanding of the *in vivo* process of copper uptake and transfer by copper chaperones.

EXPERIMENTAL PROCEDURES

Materials—Iodoacetamide (IAA)[1] was purchased from Sigma; $Na_2{}^{34}SO_4$ was purchased from ICON Stable Isotopes. HEPES and glucose were purchased from Fluka. Isopropyl-β-thiogalactopyranoside was purchased from Eurogentec. Dithiothreitol was purchased from Promega. All other materials were purchased from E. Merck AG, Darmstadt, Germany.

Bacterial Strains and Plasmids—*Escherichia coli* strain JM109 was used for cloning and expression of the *P. aeruginosa azu* gene. For the expression of the N42C and H117G azurin, the JM109 cells were transformed with the plasmids pIA02 (7) and pGKH117G, respectively. Plasmid pGKH117G was constructed by cloning the 390-bp *Sma*I-*Hin*dIII fragment of pTB46 (4, 6) into *Sma*I-*Hin*dIII-digested pGK22 (which was a kind gift from B. G. Karlsson, Chalmers University of Technology, Göteborg, Sweden). The construction of plasmid pIA03, containing both mutations (H117G and N42C) was accomplished by insertion of the 421-bp *Eco*RI-*Xma*I fragment of pIA02 containing the N42C mutation into the *Eco*RI-*Xma*I digested fragment of pGKH117G, containing the H117G mutation. Sequence analysis of the complete *azu* gene confirmed the mutations. Plasmid pIA03 was used for the expression of H117G/N42C azurin.

Protein Expression and Purification—Proteins were expressed, isolated, and purified in their apo forms as described previously (4, 7). ^{34}S-Labeled H117G/N42C azurin was isolated from JM109 cells grown on minimal medium based on a 100 mM sodium phosphate/citrate buffer, pH 7, containing 0.3% glucose, 12 mM NH_4Cl, 10 mM KCl, 1 mM $MgCl_2$, 1% thiamine (0.5 ml/liter), 50 mg/liter $Na_2{}^{34}SO_4$, 2 ml/liter mineral salts solution, and 50 μg/liter ampicillin (8). The mineral salts solution was prepared in 0.1 M HCl; sulfates were omitted and replaced by chlorides. Expression of the azurin was induced after 6.5 h of growth by the addition of 0.5 mM isopropyl-β-thiogalactopyranoside. After continuation of growth for 16 h, cells were harvested, and the ^{34}S-labeled H117G/N42C azurin was isolated using the same purification procedure as for unlabeled H117G/N42C azurin.

* This work was supported by North Atlantic Treaty Organization Grant CRG 930170, National Institutes of Health Grant GM-18865 (to J. S.-L.), The Netherlands Foundation for Chemical Research, The Netherlands Organization for Scientific Research, and Unilever Research Vlaardingen (to G. W. C. and M. v. d. B.). The costs of publication of this article were defrayed in part by the payment of page charges. This article must therefore be hereby marked "*advertisement*" in accordance with 18 U.S.C. Section 1734 solely to indicate this fact.

¶ To whom correspondence should be addressed. Tel.: 31-71-527-4256; Fax: 31-71-527-4349; E-mail: canters@chem.leidenuniv.nl.

[1] The abbreviations used are: IAA, iodoacetamide; MES, 2-(*N*-morpholino)ethanesulfonic acid; mT, millitesla.

This is an Open Access article under the CC BY license.

Gel Filtration and Mass Spectrometry—Gel filtration was performed on a Superdex 75 (Amersham Biosciences) column (60 × 1.6 cm, inner diameter), which was connected to a fast protein liquid chromatography system (Amersham Biosciences). A solution of 20 mM HEPES, 50 mM Na_2SO_4, pH 7, was used as elution buffer. For electrospray mass spectrometry, samples were exchanged to water using ultrafiltration and diluted in 50:50 water:methanol and 1% acetic acid.

UV-visible Spectroscopy—UV-visible absorption spectra were recorded at 20 °C on either a Shimadzu UV-2101 PC or a PerkinElmer lambda 18 spectrophotometer. The extinction coefficient of the absorption at 385 nm in H117G/N42C azurin has been estimated from the ratio of the absorptions at 385 nm of the Cu-H117G/N42C azurin and 280 nm of the H117G/N42C apoazurin. For the extinction coefficient at 280 nm the value of H117G apoazurin has been used ($\epsilon_{280} = 9.1 \times 10^3$ M^{-1} cm^{-1}) (9). Samples were measured in 20 mM HEPES, pH 7, unless stated otherwise.

EPR Spectroscopy—EPR spectra were recorded at 77 K with a JEOL JESRE2X spectrometer operating at X-band frequency (within a range of 8.997 and 9.000 GHz) and interfaced with a JEOL ES-PRIT330 data manipulation system. EPR spectra were recorded in continuous wave mode with instrument settings as follows: center field, 290 mT; sweep width, 75 mT; field modulation width, 1 mT; field modulation frequency, 100 kHz; time constant, 0.1 s; sweep rate, 12.5 mT/min; microwave power, 1 mW. The magnetic field was calibrated with an external sample of 1,1-diphenyl-2-picrylhydrazyl ($g = 2.0036$). Protein samples were freshly prepared by adding 0.5 molar eq of a $Cu(NO_3)_2$ solution (10 μl 25 mM) to H117G/N42C apoazurin (200 μl 2.5 mM in 20 mM HEPES buffer, pH 7, with 40% glycerol). After mixing by pipetting back and forth the solution was immediately frozen, and the EPR spectrum was measured. Subsequently, the sample was quickly defrosted to add another 0.5 molar eq of $Cu(NO_3)_2$ and measure the EPR spectrum following the same procedure.

Resonance Raman Spectroscopy—H117G/N42C apoazurin at a concentration of 0.3 mM in 20 mM HEPES, pH 7.5, and 5 mM dithiothreitol (to prevent formation of dimers) was reconstituted with Cu(II) as follows. All buffers and solutions were flushed with argon for 30 min before use. Dithiothreitol was removed by repeated dilution and concentration under anaerobic conditions. Concentrating the sample was performed in a Centricon 10, which was loaded into a Nalgene 250-ml centrifuge bottle with an O-ring sealing cap in the glove box and then centrifuged for 1.5 h at 5,000 rpm. After addition of 1 molar equivalent of $Cu(NO_3)_2$ the samples were concentrated to a final concentration of 3 mM. The samples were then inverted, spun into an Eppendorf, and transferred aerobically to capillary tubes for the measurement of absorption and resonance Raman spectra. The resonance Raman spectra of H117G/N42C azurin were collected in a 90° geometry with the capillary mounted in a wiggler (to minimize photodamage) with a stream of ice-cooled N_2 gas. For recording the spectra a custom McPherson 2061/207 spectrograph (0.67 m, 2400 groove grating) and a Princeton Instruments (LN-1100PB) liquid N_2 cooled CCD detector was used with a 150-μm slit width. Rayleigh scattering was attenuated with a Kaiser optical holographic supernotch filter. The excitation source was provided by a Coherent Innova 302 krypton laser for 413 nm (25 mW power). Absolute frequencies, accurate to at least ± 1 cm^{-1}, were obtained by calibration with aspirin. The sample was stable toward laser irradiation, and Raman spectra on the same sample could be recorded for 1.5 h.

Stopped Flow Spectroscopy—Kinetic measurements were performed on an Applied Photophysics SX.18MV stopped flow spectrometer equipped with either a PD.1 Photodiode Array detector or an absorption photomultiplier (for single wavelength). Reactions were carried out aerobically at 20 °C in 20 mM HEPES, pH 7. Reactions were initiated by mixing equal volumes of the apoazurin (50–100 μM) and a Cu(II) solution. Copper solutions were made from a 0.5 M stock solution of $Cu(NO_3)_2$. Data were analyzed with PC Pro-K, Global Analysis and Simulation Software (Applied Photophysics).

Modeling—Modeling was started by taking the crystal structure of wild type azurin and replacing His^{117} for a glycine and Asn^{42} for a cysteine using Swiss-Pdb Viewer version 3.51.[2] Using the GROMACS simulation package (11) and GROMOS 43a2 force field (12) Cys^{42} was moved inward in nine steps by putting a restraint on the distance between copper, which was constrained to sulfur(Cys^{42}) at 2.2 Å, and a dummy atom, which was placed at the average position between sulfur(Cys^{112}) and nitrogen(His^{46}). Alternately, the sulfur(Cys^{112}) and nitrogen(His^{46}) atoms were fixed, whereas the distance restraint between copper and the dummy atom was shortened; or the copper atom was fixed, and the protein was allowed to relax. Each step was run for 20 ps. After nine steps the copper-dummy distance had decreased from 12 to 1 Å. Subsequently, bonds were added between copper and the ligands (Cys^{42}, His^{46}, Cys^{112}, and Met^{121}), but they were not constrained (input distance parameters were 2.0 Å for copper-nitrogen and 2.2 Å for copper-sulfur bonds with force constants of 10^5 kJ/mol·nm^4). An improper dihedral between the copper and His^{46} was added to ensure that the copper remained in the plane of the imidazole ring (ideal improper dihedral angle: 0° with force constant of 500 kJ/mol·rad^2). During a 1.1-ns molecular dynamics run the structure appeared to be stable (root mean square deviation = 1.8 Å for all heavy atoms relative to structure at 100 ps). Water was not included in this simulation.

[2] N. Guex, M. C. Peitsch, T. Schwede, and A. Diemand (1996) Swiss-Pdb Viewer 3.51, www.expasy.ch/spdbv/mainpage.html.

RESULTS

UV-visible Spectroscopy—When Cu(II) is added to a solution containing H117G apoazurin (single mutation), the mixture turns green (4–6). The absorption spectrum of Cu-H117G azurin, taken after about 30 min when the maximum intensity in absorption is reached, is shown in the *inset* of Fig. 1*A* (*solid line*). Two absorption maxima at 420 and 628 nm are observed because of a mixture of type 2 and type 1 species, respectively (5, 6). Because water is the most abundant ligand present, it has been assumed that water coordinates the copper at the vacant position of His^{117} (5, 6), which was later shown to be correct (13, 14). The optical spectrum changes dramatically upon addition of external ligands: the addition of imidazole (and derivatives), pyridine (and derivatives), chloride or bromide to the oxidized form of the H117G mutant restores the characteristic type 1 features. For example, when imidazole is added a decrease in intensity at 420 nm and an increase near 630 nm is observed as shown in the *inset* of Fig. 1*A* (*dashed line*). Molecules such as histidine and histamine create copper sites with spectroscopic features characteristic of type 2 copper sites, as in H117G(H_2O) (4–6).

Cu(II), when added to the colorless monomeric form of the H117G/N42C apoazurin, reacts instantaneously with the protein as can be seen from the immediate development of a yellow color. This color is caused by a strong absorption band in the optical spectrum at 385 nm with an extinction coefficient of $(3.0 \pm 0.5) \times 10^3$ M^{-1} cm^{-1} (Fig. 1*A*) and is characteristic of a type 2 copper site. It can be assigned as a $RS^- - Cu(II)$ $\sigma \rightarrow \pi^*$ band (15–18). These features are strikingly different from the spectroscopic characteristics of Cu-H117G azurin mentioned above (Fig. 1*A*, *inset*, *solid line*). Remarkable is that the addition of an excess of external ligands such as imidazole (50 eq) or chloride (100 eq) *after copper binding* does not influence the spectroscopic features (*dashed lines* in Fig. 1, *B* and *C*, respectively). Preincubation with a large excess of imidazole before Cu(II) is added slightly affects the spectroscopic properties. An increase in absorption at 630 nm is observed as well as a slight decrease in 385 nm absorption. The gain in 630 nm absorption agrees stoichiometrically with the loss of 385 nm absorption as calculated from the extinction coefficients of 385 nm ($(3.0 \pm 0.5) \times 10^3$ M^{-1} cm^{-1}) and 628 nm ($(5.3 \pm 0.1) \times 10^3$ M^{-1} cm^{-1}, imidazole-bound H117G azurin (9)) (Fig. 1*B*, *dotted line*). Preincubation with chloride has hardly any effect on the spectroscopic features (Fig. 1*C*, *dotted line*). These observations are in contrast to H117G azurin, which changes its spectroscopic properties dramatically upon adding exogenous ligands as depicted in Fig. 1*A* (*inset*, *dashed line*). From this, it can be concluded that in the case of H117G/N42C azurin externally added ligands do not significantly compete for copper binding. The open site in the coordination sphere of the copper, therefore, must be occupied by another ligand, the obvious candidate being Cys^{42}.

The involvement of cysteine 42 in copper binding was confirmed by inhibition studies with IAA, a blocking reagent that

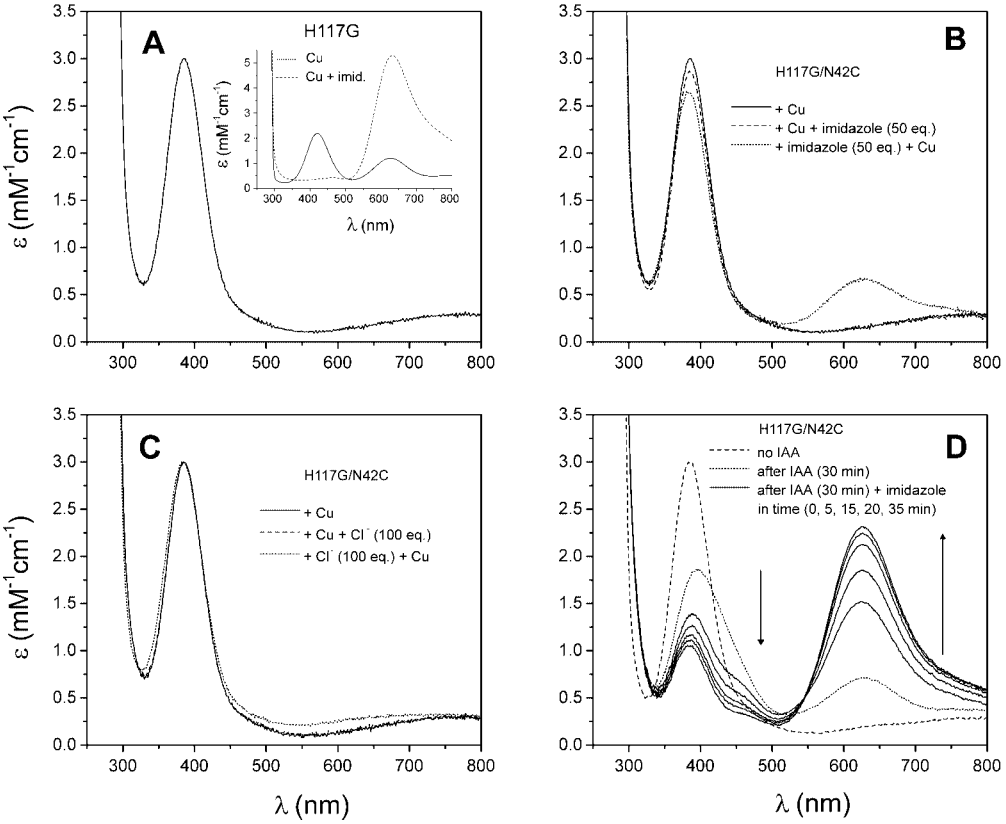

FIG. 1. **UV-visible spectra of H117G/N42C azurin monomer and inhibition studies.** Spectra were taken in 20 mM HEPES, pH 7, at 20 °C; H117G/N42C azurin samples were at protein concentrations of 30 μM. *A*, Cu-H117G/N42C azurin. *Inset*, Cu-H117G azurin; *solid line*, 0.1 mM in 20 mM HEPES, pH 7, at 20 °C; *dashed line*, imidazole-reconstituted Cu-H117G azurin. *B*, effect of imidazole. *Solid line*, Cu-H117G/N42C azurin; *dashed line*, Cu-H117G/N42C azurin after addition of 50 eq of imidazole; *dotted line*, Cu-H117G/N42C azurin after preincubation of H117G/N42C apoazurin with 50 eq of imidazole. *C*, effect of chloride. *Solid line*, Cu-H117G/N42C azurin; *dashed line* (which coincides with the *solid line*), Cu-H117G/N42C azurin after the addition of 100 eq of NaCl; *dotted line*, Cu-H117G/N42C azurin after preincubation of H117G/N42C apoazurin with 100 eq of NaCl. *D*, partial IAA inhibition (70%). *Dashed line*, Cu-H117G/N42C azurin; *dotted line*, Cu-H117G/N42C azurin after preincubation of H117G/N42C apoazurin with 10 eq of IAA for 30 min; *solid lines*, Cu-H117G/N42C after preincubation with IAA and addition of 3.3 eq of imidazole followed in 0, 5, 15, 20, and 35 min.

reacts specifically with surface-exposed cysteine residues. The addition of copper after preincubation of the apo monomer of H117G/N42C azurin with IAA restores the characteristic properties of the H117G mutant as shown in Fig. 1*D*. Depending on (*a*) the amount of IAA used, (*b*) the protein concentration, (*c*) the incubation time, and (*d*) the temperature, the absorption at 385 nm decreases to a smaller or larger extent, whereas the absorptions at 420 and 630 nm, typical for Cu-H117G azurin, increase (Fig. 1*D*, *dotted line*). Under the conditions as used in Fig. 1*D* about 70% of the Cys^{42} in the H117G/N42C apoazurin has reacted with IAA after 30 min, making binding of this cysteine to the copper impossible. The *dotted line* in Fig. 1*D* (after IAA) has decreased relative to the *dashed line* (no IAA); the apparent slight shift of the absorption maximum to longer wavelength is caused by overlap of the remaining 385 nm absorption with the newly appearing 420 nm absorption. Thus, the original green copper site as observed for the H117G azurin mutant is partially recovered. A free position has become available in the coordination sphere of the metal site, which can be filled by externally added ligands: upon adding imidazole a decrease in 420 nm absorption and an increase in 630 nm absorption are observed (*solid lines*, Fig. 1*D*). Under the conditions used in Fig. 1*D*, a remaining absorption at 385 nm is observed caused by the presence of H117G/N42C azurin that has not reacted with IAA (about 30%).

Dimer Formation—Previous studies have demonstrated that the addition of Cu(II) (1.1 molar eq) to the apo form of the N42C single mutant catalyzes the formation of dimers (7). The copper occupies the metal site but is partially reduced as it participates in the oxidation of the cysteines 42 when they form a disulfide bond. It is thus expected that copper addition to the H117G/N42C double mutant will result in the accelerated formation of dimers. To analyze this feature an experiment was performed, in which 1.1 molar eq of Cu(II) was added to apo monomer of H117G/N42C azurin. The resulting yellow protein solution was subjected to size exclusion column chromatography. From this, two fractions were eluted with masses of 13,853 ± 2 and 27,698 ± 4 Da, respectively, as determined by mass spectrometry. This agrees with the expected mass of the apo forms of mono- and dimer, calculated as 13,852 and 27,702 Da, respectively.[3] The experiment shows that during a gel filtration experiment at least 20% of the total amount of protein is converted into a dimer, independent of the protein concentration. We found that at high protein concentrations and longer incubation times, up to 80% of the total amount of monomer could be dimerized at ambient temperatures.

The eluted monomer fraction still shows absorption at 385 nm, demonstrating that the yellow compound is a monomeric form of the protein, and excluding the occurrence of a possible dimer, in which a cysteine of one monomer ligates to the copper of the other monomer. The eluted dimer fraction was colorless, compatible with the copper being in the reduced state. The copper could not be reoxidized with potassium ferricyanide to

[3] Under the acidic conditions used for electrospray mass spectrometry, the copper falls out (see also Ref. 58).

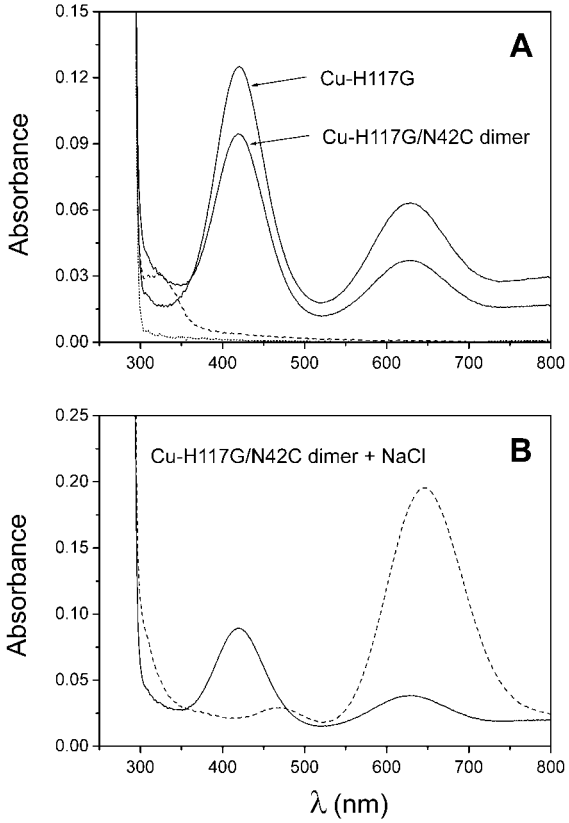

FIG. 2. **UV-visible spectra of H117G/N42C azurin dimer.** Spectra were taken in 20 mM MES, pH 6, at 20 °C. Samples were at a protein concentration of 55 μM. *A*, H117G/N42C apoazurin dimer (*dashed line*) and H117G apoazurin (*dotted line*) reconstituted with a stoichiometric amount of $Cu(NO_3)_2$/copper site (*solid lines* as indicated). *B*, Cu-H117G/N42C dimer (*solid line*) after the addition of 1 M NaCl (*dashed line*) resulting in the appearance of a blue type 1 copper site as in H117G azurin (analogous to Fig. 1*A*, *inset*).

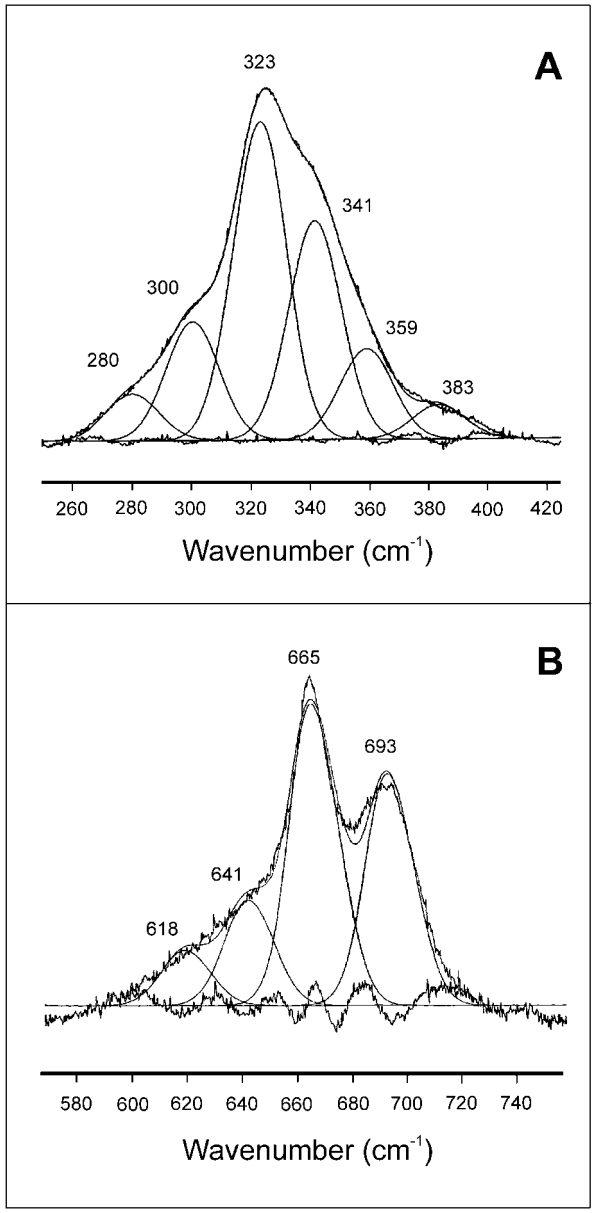

FIG. 3. **Resonance Raman spectrum of H117G/N42C azurin at pH 7.5 with deconvolutions.** *A*, low frequency range (fundamentals). *B*, high frequency range (combination bands). The spectrum was obtained using 413 nm excitation (25 mW), spectral resolution of 1 cm^{-1}, and 30 min of data collection. The Raman spectrum of the apoprotein was subtracted to remove the protein and glass contribution. Curves were fitted with (Gaussian) peak widths at a half-height of 21 cm^{-1}. The individual peaks and the sum of the individual peaks as well as residuals are shown.

the Cu(II) form as could have been expected for a H117G azurin variant (6, 9). The possibility for the dimer being in its apo form is not likely because reconstitution with copper could not be achieved. The possibility of partial oxidation of the cysteine sulfur preventing binding of copper, however, cannot be ruled out. The possibility of zinc, instead of copper, occupying the metal site is ruled out because Zn-H117G/N42C azurin was removed prior to the gel filtration experiment by anion exchange chromatography.

The formation of disulfide dimers of H117G/N42C azurin also occurs by exposure to air, in the absence of copper. This apo dimer can be reconstituted with copper by the addition of a stoichiometric amount of Cu(II) per copper site. Addition of Cu(II) to the apo dimer produces a green color with an absorption spectrum that is identical to that of the H117G single mutant (Fig. 2*A*, *solid lines*), although the intensities of absorbances of the double mutant are slightly lower (the absorbances at 420 and 630 nm amount to 76 and 57% of the H117G absorbances, respectively). Thus, upon the formation of the disulfide bond, the cysteines 42 are no longer available for copper binding, and the original spectroscopic features of the H117G mutant are restored. Just as with H117G azurin the vacant position can be filled by external ligands such as imidazole and chloride resulting in the appearance of a blue type 1 copper site (Fig. 2*B*). In addition, a weak absorption band around 320 nm is observed, which is also present in the apoprotein (Fig. 2*A*, *dashed line*). This feature might be related to the decreased intensity at 420 and 630 nm (see "Discussion").

Resonance Raman Spectroscopy—The resonance Raman spectrum of the yellow monomeric form of H117G/N42C shows fundamentals at 300, 323, 341, and 359 cm^{-1} which originate from modes involving the Cu-S(Cys) stretching vibration (Fig. 3*A*), similar to the spectra of copper cysteinates (Table I) with tetragonal type 2 copper sites, like the His → Gly mutants of azurin (5, 19–21) and various superoxide dismutase mutants (19, 22). In addition, higher frequency vibrations are observed at 665 and 693 cm^{-1}, which are assigned as combination bands of the 341 cm^{-1} fundamental with the 323 and 359 cm^{-1} vibrations, respectively (Fig. 3*B*). Weaker are the vibrational modes at 618 and 641 cm^{-1}, which can be assigned as combination bands of the 300 cm^{-1} fundamental with the 323 and 341 cm^{-1} vibrations, respectively. There are no strongly enhanced overtone bands or S-C stretch vibrations of cysteine

TABLE I
Resonance Raman frequencies of type 2 copper proteins
Spectra were obtained with 413 nm excitation. Frequencies in boldface denote the most intense peak(s) in the spectrum.

Protein	λ_{max}	Fundamentals							Combination bands	
	nm	*cm*$^{-1}$							*cm*$^{-1}$	
H117G/N42C azurin	385		300	**323**	**341**	359			665	693
H117G azurin (His)[a]	400	259	**296**	**319**	350		388			
H117G azurin (H_2O)[b]	420	267	**298**	**317**	352	362	387	404		
H46G azurin (imidazole)[c]	380	261	295	**325**	337	353	388			
H46G azurin (H_2O)[c]	400	267	295	**330**	339		392	403		
SOD-H46C (Cu_2Zn_2) (pH 5.5)[d]	379	271	298	320	**342**		378			
SOD-H120C (Cu_2Zn_2)[d]	406	283			341	**359**	**366**	401		
SOD-H80C (Cu_2Cu_2) (yellow)[d]	411	283	292	335	**348**			403		
SOD-H46R[e]	370			322	**348**	**357**		407	675	698
Cu-LADH (imidazole)[f]	480		**306**	**325**	336	364		411	ND	ND

[a] Refs. 19 and 20.
[b] Ref. 5.
[c] Ref. 21.
[d] Ref. 19. SOD, superoxide dismutase.
[e] Ref. 22.
[f] Spectrum was obtained with 514.5 nm excitation; Ref. 36. ND, not determined LADH, liver alcohol dehydrogenase.

present. However, the predominance of combination bands in the higher frequency region is typical of Cu-S(Cys) chromophores.

To demonstrate the involvement of two cysteine ligands (Cys^{42} and Cys^{112}) in copper coordination ^{34}S-labeled H117G/N42C azurin was produced to identify multiple Cu-S stretching modes by their high frequency shifts. This method has been applied successfully for example in the study of the dinuclear copper cysteinate sites (Cu_A in cytochrome *c* oxidase and N_2O reductase) (23–26). However, the ^{34}S-labeled H117G/N42C azurin could be reconstituted with copper only to a very small extent, most probably because for the majority of the azurin molecules oxidative damage of the thiol group of Cys^{112} had occurred (see below). Interestingly, the UV-visible spectrum of the ^{34}S-labeled H117G/N42C azurin showed a strong increase in absorption around 320 nm (Fig. 4*A*). Furthermore, the mass spectrum showed multiple peaks all differing from the parent compound by multiples of 16 on average, corresponding with the mass of one oxygen (Fig. 4*A*, *inset*; the calculated mass of the unmodified ^{34}S-labeled H117G/N42C azurin equals 13,872 Da). It appears that the absorption at 320 nm in the optical spectrum is related to the degree of oxidation in the sample as determined by mass spectrometry. Samples with a relatively high absorption around 320 nm show mass spectra with a high degree of oxidation products resulting for example from the oxidation of cysteine thiols giving products such as sulfonic (Cys-SOH) or sulfinic acid (Cys-SO_2H), or the oxidation of the thioether sulfurs of methionines giving products such as sulfoxides (Met-SO) or sulfones (Met-SO_2) or the oxidation of the Cys^3-Cys^{26} cystine to various extents, *i.e.* monooxo, dioxo, trioxo, tetraoxo, pentaoxo, and the fully oxidized form (27, 28). In contrast, samples without absorption at 320 nm give a single peak with the expected mass as shown for a ^{32}S-H117G/N42C azurin sample (Fig. 4*B*, calculated mass of 13,852 Da).

Kinetics of Copper Incorporation—The absorption at 385 nm which appears upon addition of copper to the apo monomer of H117G/N42C azurin, reaches its maximum when 1 eq of copper is used. Addition of more than 1 eq of copper does not increase the absorption any further (Fig. 5), indicative of a strong binding site with one copper per monomer. Remarkable is that at copper/protein ratios lower than 1 the wavelength of the absorbance maximum (measured after 2 min) is slightly shifted to higher energies (see *inset*, Fig. 5). With time, the peak maximum shifts to 385 nm.

To examine the mechanism of copper uptake of the H117G/N42C apoazurin monomer, stopped flow UV-visible spectroscopy was performed. Multiple phases can be distinguished on

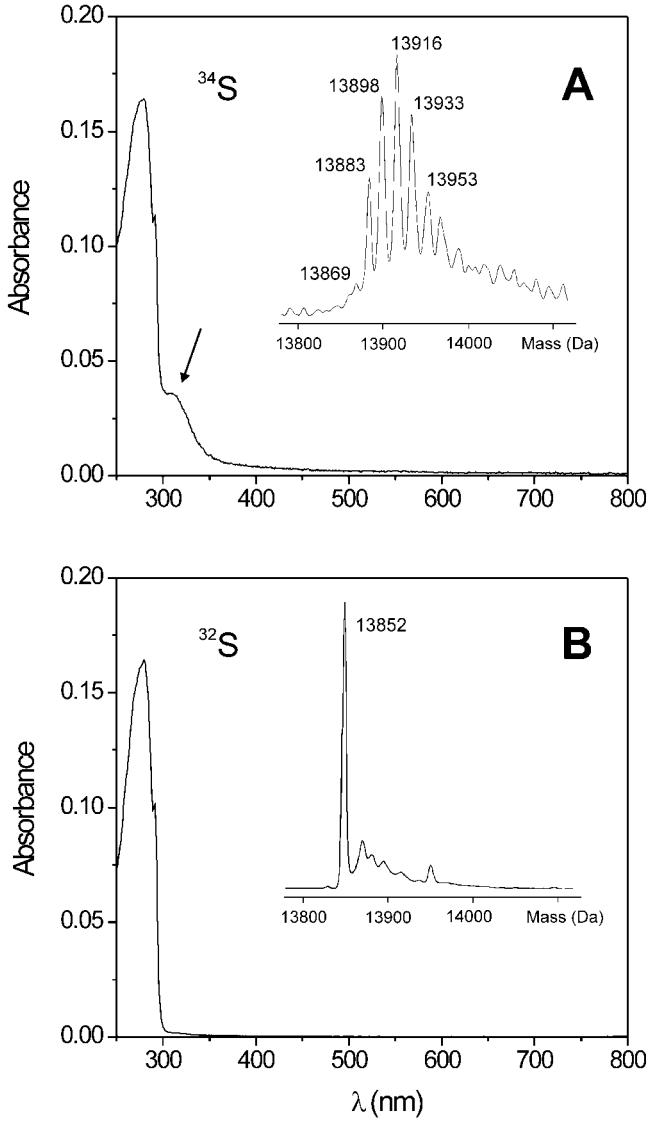

FIG. 4. **UV-visible spectra and reconstituted molecular weight profile of electrospray mass spectra (*insets*) of H117G/N42C apoazurin.** UV-visible spectra were taken in 20 mM HEPES, pH 7, at 20 °C; protein concentrations were 20 μM. Note the intensity of the 320 nm absorption (*arrow*) and the high degree of oxidation of the protein (mass spectra). *A*, ^{34}S-H117G/N42C apoazurin. *B*, ^{32}S-H117G/N42C apoazurin. The calculated masses of ^{34}S-H117G/N42C apoazurin and ^{32}S-H117G/N42C apoazurin are 13,872 and 13,852 Da, respectively.

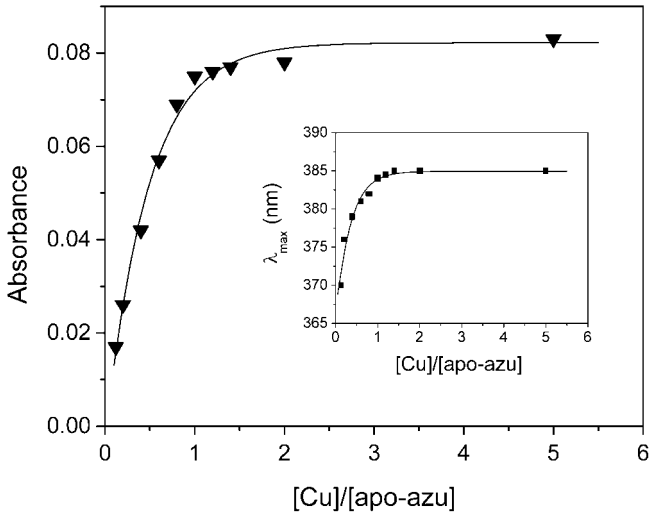

FIG. 5. **Reconstitution of H117G/N42C apoazurin with $Cu(NO_3)_2$.** H117G/N42C apoazurin in 20 mM HEPES, pH 7, was mixed with small amounts of a 10 mM $Cu(NO_3)_2$ solution at 20 °C. The concentration of H117G/N42C apoazurin ([apo-azu]) was kept constant at 50 μM. Absorption spectra were taken 2 min after adding $Cu(NO_3)_2$. The maximal absorbance around 385 nm is plotted against the [Cu]/[apo-azu] ratio. The *inset* shows the wavelength of maximal absorbance (λ_{max}) as a function of the [Cu]/[apo-azu] ratio.

different time scales. The first step is very fast: addition of 20 eq of $Cu(NO_3)_2$ to 100 μM H117G/N42C apoazurin monomer resulted in the formation of an intermediate with an absorption maximum around 385 nm, which developed within 10 ms (Fig. 6*A*). The rate depends on the copper concentration, indicating that this is a bimolecular reaction. In the second, slower step a slight increase (10–20%) in absorption occurs as well as a shift in the absorption maximum to λ_{max} = 369 nm (Fig. 6*B*). This phase is independent of copper concentration and lasts less than 1 s. Presumably, a rearrangement takes place in which the loop containing Cys^{42} moves inside the cavity. Subsequently, the absorption starts to decrease again in several steps: 1) a decrease in absorption as well as a shift back to 385 nm within 4 s; 2) a further decrease in absorption at a time scale of 1 min (Fig. 6*C*); and 3) a further decrease in absorption at a time scale of 1 h and longer (days).

Interestingly, stopped flow data analysis of the N42C *single azurin mutant* also shows the very fast formation of a species that absorbs around 385 nm, which is then followed rapidly by the disappearance of this intermediate and the simultaneous appearance of the typical 628 nm absorption, known for type 1 copper proteins (Fig. 6*D*).

EPR Spectroscopy—EPR spectra of H117G/N42C azurin in the presence of 0.5 and 1.0 eq of copper recorded at 77 K are shown in Fig. 7, *A* and *B*, respectively. The EPR spectrum of H117G/N42C azurin with 0.5 eq of copper shows at least three species. The relatively large hyperfine coupling constants ($> 140 \times 10^{-4}$ cm^{-1}) are characteristic of type 2 copper sites. The experimental EPR conditions (temperature of 77 K) plus the addition of only 0.5 molar eq has slowed down the uptake of copper, thereby trapping the different intermediates that are formed during this process possibly corresponding with the type 2 copper intermediates observed during stopped flow spectroscopy (see above).

In the EPR spectrum of H117G/N42C apoazurin to which 1 eq of copper is added two species can be distinguished, again with type 2 copper site characteristics ($A_\parallel = 160 \times 10^{-4}$ cm^{-1}; $g_\parallel = 2.23$ and $A_\parallel = 170 \times 10^{-4}$ cm^{-1}; $g_\parallel = 2.28$). After 3 days at −20 °C the latter species has almost disappeared, leaving the more stable species ($A_\parallel = 160 \times 10^{-4}$ cm^{-1}; $g_\parallel = 2.23$) as can be seen in Fig. 7*C*. It is likely that this more stable species corresponds with the final species that absorbs at 385 nm in the optical spectrum. The intermediate absorbing at 369 nm might correspond to the species with $A_\parallel = 170 \times 10^{-4}$ cm^{-1} and $g_\parallel$ = 2.28. The third less well defined species in the EPR spectrum (Fig. 7*A*) possibly represents the first intermediate absorbing at 385 nm.

Modeling—Because the stability of the yellow species of H117G/N42C azurin is limited, structure determination with regular methods is prohibited. To obtain insight in the possible structure of this form of the protein, a model was built using molecular dynamics calculations. The calculations were not meant to simulate the formation of or to establish unequivocally the structure of the copper site. The purpose was to see whether a strain-free model of the copper site might be obtained with the most likely set of ligands and what rearrangement of the protein might be needed. The simulations were performed on the basis of the following experimental observations. The data show that cysteine 42 is acting as one of the copper ligands in a tetragonal type 2 copper site. In addition, resonance Raman spectroscopy provides a strong indication that two cysteine residues are involved (see below), which makes Cys^{112} a second ligand. Two other possible ligands are His^{46} and Met^{121}, which are coordinating to the copper in the native site. To model a copper site with these supposed ligands (Cys^{42}, Cys^{112}, His^{46}, and Met^{121}) residue Cys^{42}, with the copper ion bound to it at 2.2 Å distance, was pulled into the cavity, and the protein structure was allowed to relax (for details, see "Experimental Procedures"). The result is illustrated in Fig. 8. In Fig. 8*A* the structure of wild type azurin is shown; Fig. 8*B* shows a model of H117G/N42C azurin with Cys^{42}, Cys^{112}, His^{46}, and Met^{121} providing the copper ligands. The surface representations in Fig. 8, *C* and *D*, are viewed from above displaying the hydrophobic patch before and after the moving in of the loop (*red*) with Cys^{42} (*yellow*), respectively. From these figures it is clearly seen that the loop (residues 36–47) has rearranged, enabling Cys^{42} to participate in copper binding. Although the overall structure is stable during the molecular dynamics run (1.1 ns), there is some slight residual strain in the loop around residue 42, as residue Lys^{41} occurs in a disfavored region of the Ramachandran diagram. The participation of Met^{121} in copper binding is uncertain because the distance between $S^{\delta}(Met^{121})$ and copper stays relatively large. Preliminary results of further molecular dynamics and quantum mechanics/molecular mechanics calculations indicate that the involvement of water as a copper ligand, instead of Met^{121}, should be considered as a possibility.

DISCUSSION

Cys^{42} as a Copper Ligand—The introduction of the N42C mutation in the H117G azurin mutant causes a dramatic change in the absorption spectrum of the copper-reconstituted protein relative to H117G azurin. Instead of two absorption maxima at 420 and 630 nm, as in H117G azurin, a single absorption maximum at 385 nm is observed, which is attributed to an RS^- – Cu(II) $\sigma \rightarrow \pi^*$ band typical for type 2 copper sites. Although addition of external ligands such as imidazole and chloride changes the optical spectrum of Cu-H117G azurin dramatically, hardly any effect is observed in the case of Cu-H117G/N42C azurin. However, it turns out that blocking Cys^{42} can restore the H117G characteristics, either by reaction with IAA or by dimer formation. These observations together show that Cys^{42} is involved in copper binding in the yellow form of the double mutant.

Although it seems that Cys^{42} is far away from the copper in the three-dimensional structure, it is in fairly close proximity to the gap created by the removal of the histidine side chain

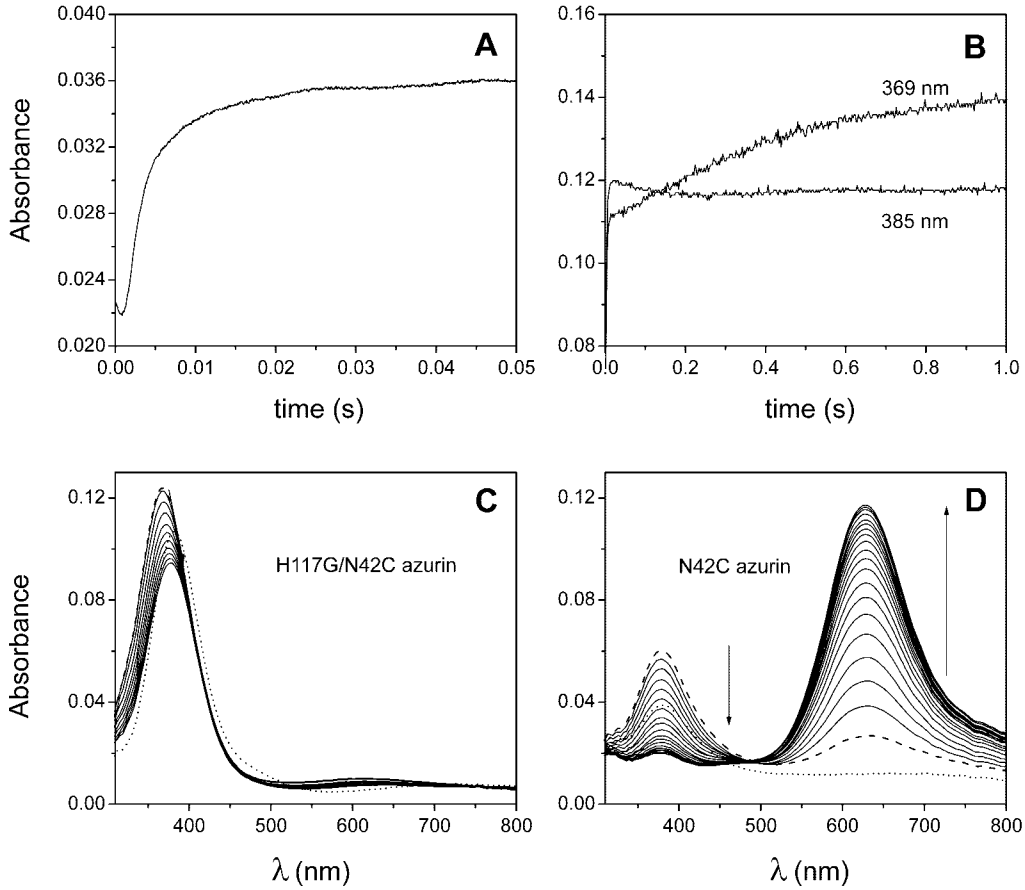

FIG. 6. **Kinetic traces of the incorporation of copper in H117G/N42C apoazurin at 20 °C, 20 mM HEPES, pH 7.** *A*, formation of first intermediate with absorption maximum at 385 nm. Concentrations of H117G/N42C apoazurin and $Cu(NO_3)_2$ are 100 μM and 2 mM, respectively. *B*, formation of second intermediate with absorption maximum at 369 nm. Absorption at 385 nm is decreased. Concentrations of H117G/N42C apoazurin and $Cu(NO_3)_2$ are 100 and 400 μM, respectively. Data are taken from kinetic profiles produced after data acquisition over the wavelength range 300–1,100 nm for 1 s (integration time, 2.56 ms). *C*, kinetic spectral profiles for the incorporation of copper of H117G/N42C azurin for the first 32 s. Concentration of H117G/N42C apoazurin and $Cu(NO_3)_2$ are 100 and 200 μM, respectively. Integration time acquisition is 0.16 s. The first spectrum taken at 0.08 s is shown as a *dotted line*. Maximal absorbance is reached after 2.4 s at λ_{max} = 369 nm (*dashed line*), which is followed by a decrease in absorption and a shift back toward 385 nm (*solid lines*). *D*, kinetic spectral profiles for the incorporation of copper of N42C azurin for the first 32 s. Concentrations of N42C apoazurin and $Cu(NO_3)_2$ are 50 and 100 μM, respectively. Integration time acquisition is 0.08 s. The first spectrum taken at 0.04 s is shown as a *dotted line*. Maximal absorbance is reached after 1.3 s at λ_{max} = 380 nm (*dashed line*), which is followed by a decrease in absorption at 380 nm and an increase in 628 nm absorption (*solid lines*).

(Fig. 8). The loops in the hydrophobic patch surrounding residue 117 have an increased mobility compared with wild type azurin (13, 27). Apparently, the loop containing residues 36–47 is flexible enough to enable Cys^{42} to move toward the cavity where it can act as a copper ligand. The fact that Cys^{42} is covalently attached to the protein framework increases its "effective concentration" with respect to copper binding and helps to increase the binding constant compared with noncovalently linked ligands.

The idea of filling a gap that has been created in the coordination sphere of a metal in a metalloenzyme has been reported for other metalloproteins, for instance in sperm whale myoglobin (29–31), iso-1-cytochrome *c* (32), and cytochrome *c* peroxidase (33) (for a review, see Ref. 34). In some cases replacement of a metal-coordinating amino acid side chain by a smaller one results in a rearrangement of the protein structure to make a new ligand available for binding which is positioned nearby. For example, mutation of Cys^{20} of *Azotobacter vinelandii* ferredoxin I, which is a ligand of the [4Fe-4S] cluster in the native protein, into an alanine results in a new [4Fe-4S] cluster that derives its fourth ligand from Cys^{24}, a free cysteine in the native protein (35). The formation of this [4Fe-4S] cluster drives the rearrangement of the protein structure. Similarly, in H117G/N42C, a rearrangement enables Cys^{42} to occupy the vacant coordination position created by the removal of the His^{117} side chain.

Resonance Raman Spectroscopy, Two Cysteinate Ligands—The resonance Raman spectrum of the yellow H117G/N42C mutant is similar to that of other copper cysteinates (Table I) with tetragonal type 2 copper sites, such as the His → Gly mutants of azurin (5, 19–21) and superoxide dismutase mutants (19, 22). The appearance of two to four fundamentals in the 295–365 cm^{-1} region is characteristic for these proteins and is regardless of whether there is a single cysteinate ligand (as in the azurin single mutants) or whether there are two cysteinate ligands (as in copper-liver alcohol dehydrogenase (36) and as suggested in superoxide dismutase H46R (22)). The observation of combination bands, however, is not observed for the single thiolate tetragonal sites of azurin and superoxide dismutase (19, 21). As in superoxide dismutase H46R (22), the combination bands in the H117G/N42C azurin are indicative of two cysteinate ligands. Such combination bands are observed in copper-substituted liver alcohol dehydrogenase (36) and other metal cysteinate proteins with multiple cysteinate ligands such as Cu_A (24, 26), rubredoxin (37), and ferredoxin (38) as well as in the copper-sulfide cluster Z_{ox} in N_2O reductase (26) (Table II).

^{34}S substitution, which can be used, in principle, to identify

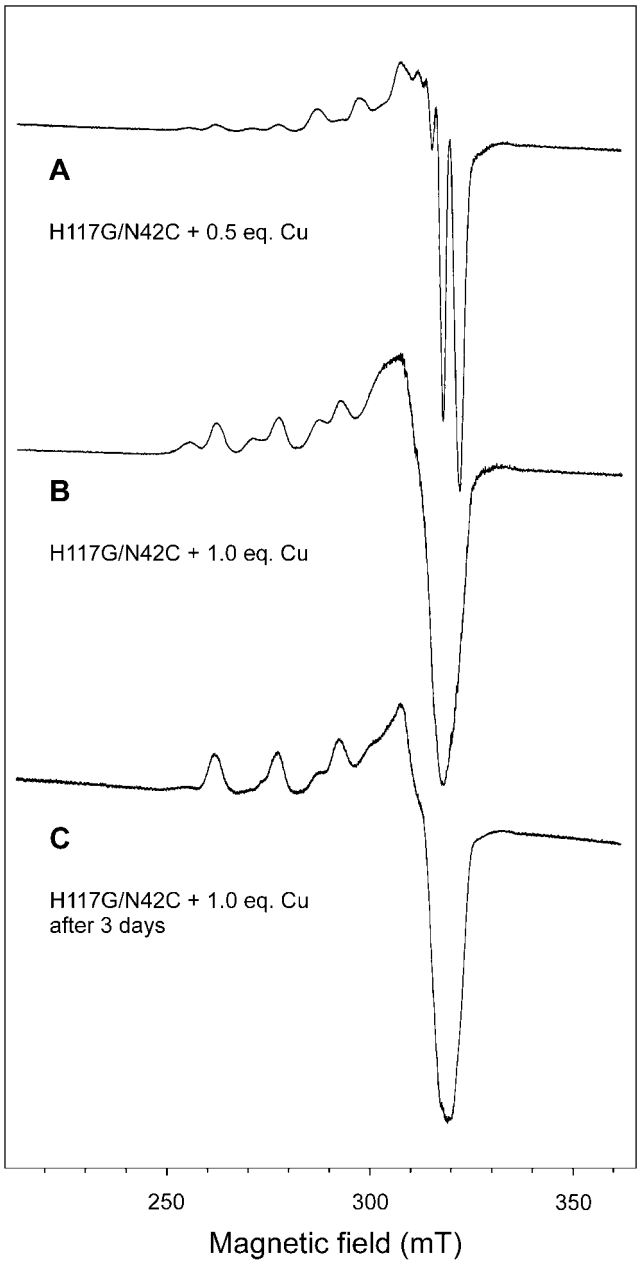

FIG. 7. **EPR spectra of 2.5 mM H117G/N42C azurin in 20 mM HEPES, pH 7, 40% glycerol at 77 K.** *A*, after the addition of 0.5 eq of $Cu(NO_3)_2$ frozen within 20 s of mixing. *B*, sample from *A* refrozen after 1 min of thawing and remixing with a total amount of 1.0 eq of $Cu(NO_3)_2$. *C*, sample from *B* after 3 days at −20 °C. All copper signals in *A–C* represent protein-bound copper; no signal is observed from inorganic copper.

multiple Cu-S stretching modes, was not successful. The binding of copper in the active site was inhibited because of the oxidative conversion of the sulfur cysteines and/or methionines into $S(O)_n$ in the ^{34}S-substituted H117G/N42C. The possibility of such a modification of the Cys^{112} sulfur is supported by crystallographic data on the H117G azurin, which show that Cys^{112} can be oxidized leading to the loss of copper (27). Because the Cys^{112} residue is relatively exposed in the apo form it is likely that in the H117G/N42C azurin not only the highly exposed Cys^{42}, but also Cys^{112} is oxidized. The degree of oxidation appears to be related to the absorption around 320 nm in the optical spectrum (Fig. 4). The extensive oxidation of ^{34}S-labeled H117G/N42C in the bacteria likely results from the oxidative stress during the relatively long aerobic growth conditions on minimal medium (39–44). The same oxidation pattern was observed for ^{32}S-H117G/N42C azurin when grown on minimal medium. Slight oxidation of ^{32}S-H117G/N42C azurin (grown on rich medium) during storage may explain the small variations in intensity of the 385 nm absorption observed for the yellow compound as well as the less intense 420 and 630 nm absorption bands in the H117G/N42C dimers compared with H117G azurin.

Copper Incorporation—The monomeric form of the H117G/N42C azurin exhibits very intriguing kinetics of copper uptake. The first step is very fast: under pseudo-first order conditions an intermediate is formed within 10 ms with an absorption maximum at 385 nm, indicative of a $RS^- - Cu(II)$ $\sigma \rightarrow \pi^*$ band in a Cu(II)-thiolate center with a tetragonal geometry (15–17). The formation of such an intermediate has been observed during the incorporation of copper in a Cu_A azurin (45). Upon addition of Cu(II) to the apoprotein an intermediate containing a tetragonal Cu(II)-S(Cys) center was identified, characterized by an absorption around 386 nm which developed within 10 ms, similar to our case.

Interestingly, stopped flow data analysis of the N42C *single mutant* of azurin also shows the very fast formation of a species that absorbs around 385 nm, which is then followed rapidly by its disappearance and the simultaneous appearance of the typical 628 nm absorption, known for type 1 copper proteins (Fig. 6*D*). The formation of the yellow intermediate is not observed in wild type azurin (46–48). Apparently, the surface-exposed cysteine in the N42C mutant is responsible for the development of the intermediate species. Previously, it has been concluded that the incorporation of copper in wild type apoazurin is accomplished by a mechanism by which His^{117} scavenges the Cu(II) from the solution and thus effectively increases the local concentration of the Cu(II) in the vicinity of the metal binding site (swinging door mechanism (46, 47, 49)). The high affinity of copper for cysteines together with the fact that Cys^{42} in N42C azurin is even more exposed than His^{117} is in agreement with the cysteine taking over the role of His^{117} in picking up the copper from the solution. In the case of the H117G/N42C azurin the Cys^{42} subsequently transfers the copper to the metal binding site inside the protein by a rearrangement of the protein and is able to act as a ligand itself. In the N42C variant the His^{117} is still present, and no space is available for Cys^{42} to adopt a copper-coordinating role amid the regular copper ligands.

The findings described here show similarities with the way copper chaperones bind and transfer their copper ions in the living cell, although copper is bound as Cu(I) instead of Cu(II) in these cases. Proposed mechanisms for the exchange of Cu(I) involve both two- and three-coordination geometries in which at least two thiolate ligands are involved. Copper binding induces a conformational change that is followed by the transfer of copper by ligand exchange involving amino acids in or near the metal binding site of the target protein (for reviews, see Refs. 50–55).

The study of the copper incorporation into H117G/N42C apoazurin shows that different intermediates can be distinguished at different time scales. At low temperature the copper incorporation is slowed down, and consequently, intermediates, which all show type 2 characteristics, can be trapped as demonstrated by the EPR data. The experimental observations fit into a scheme whereby in the first step Cys^{42} scavenges the Cu(II) from the solution. This leads to the formation of an intermediate tetragonal Cu(II)-S(Cys^{42}) center, displaying a strong absorption at 385 nm. Subsequently, this intermediate converts into a second longer lived intermediate (with an absorption maximum at 369 nm) by the rearrangement of the loop

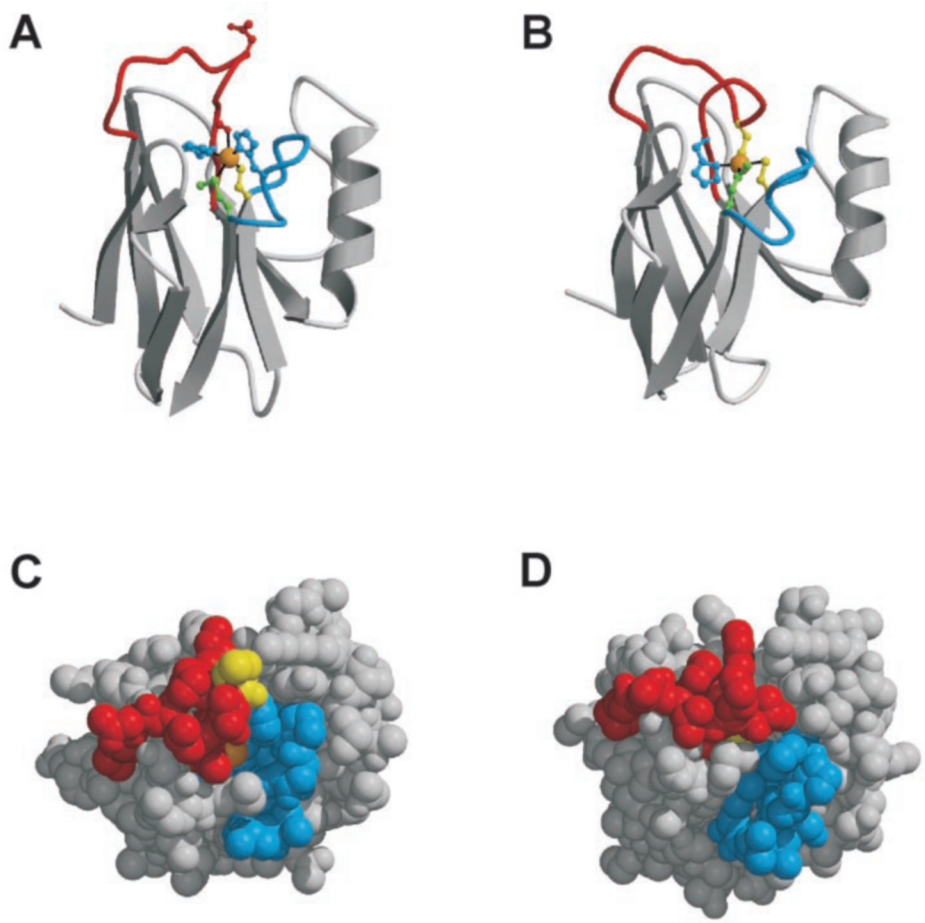

FIG. 8. **Modeling of yellow form of H117G/N42C azurin.** *A*, representation of wild type azurin, showing loops with residues 36–47 and 112–121 in *red* and *blue*, respectively. The side chains of copper ligands His^{117}, His^{46} (both in *blue*), Cys^{112} (*yellow*), Met^{121} (*green*) and the backbone oxygen of Gly^{45} as well as Asn^{42} (both in *red*) are shown in *ball and stick* representation. Copper is depicted as an *orange sphere*. *B*, modeled structure of H117G/N42C azurin, in which Cys^{42} (*yellow*) has moved inward to act as a copper ligand. Together with the other ligands, Cys^{112} (*yellow*), His^{46} (*blue*), and Met^{121} (*green*), a tetragonal copper site is formed. Orientation is similar to that in *A*. *C*, space-filled model of H117G/N42C azurin viewed perpendicular to the hydrophobic patch before modeling. The structure is as wild type azurin (*A*) with Asn^{42} replaced by Cys (*yellow*) and His^{117} replaced by Gly, which makes the copper (*orange*) accessible to the outside. Loops with residues 36–47 and 112–121 are shown in *red* and *blue*, respectively. *D*, space-filled model of H117G/N42C azurin after modeling (as in *B*) viewed perpendicular to the hydrophobic patch. *Colors* are as in *C*. All images were generated with MOLSCRIPT (59) and RASTER3D (10).

TABLE II
Combination bands in resonance Raman spectra of metal cysteinate proteins

Metal site	Combination band 1	Combination band 2
	cm^{-1}	cm^{-1}
$Cu(Cys)_2$		
H117G/N42C azurin	665 (341 + 323)	693 (341 + 359)
SOD-H46R[a]	675 (357 + 322)	698 (357 + 348)
$Cu_2(Cys)_2$		
Cu_A of CCO[b]	598 (260 + 339)	680 (339 + 339)
Cu_A of N_2O reductase[c]	602 (259 + 347)	684 (347 + 347)
$Fe(Cys)_4$		
Rubredoxin[d]	627 (314 + 314)	689 (314 + 376)
$Fe_2(S)_2(Cys)_4$		
Ferredoxin[e]	563 (282 + 282)	650 (282 + 367)
	622 (282 + 339)	675 (339 + 339)
Cu_4S		
Z_{ox} of N_2O reductase[c]	691 (347 + 347)	755 (347 + 408)

[a] Ref. 22. SOD, superoxide dismutase.
[b] Ref. 24. CCO, cytochrome *c* oxidase.
[c] Ref. 26.
[d] Ref. 37.
[e] Ref. 38.

containing Cys^{42}. Finally, the absorption maximum shifts back to 385 nm, completing the formation of the copper site by ligation of Cys^{112}, and possibly, His^{46} and Met^{121}, which are the regular copper ligands in the native site.

Because the rate of the formation of the first intermediate depends on the copper concentration, the rate of formation of subsequent intermediates also depends indirectly on the copper concentration. This effect is clearly seen in Fig. 5, where at a copper/protein ratio lower than 1 the formation of the final copper site after 2 min is not completed, and the absorption maxima have not reached their final position at 385 nm. The decrease in absorption after the formation of the second intermediate (Fig. 6*C*) most likely results from the formation of dimers. As shown previously, disulfide formation results in the reduction of Cu(II) to Cu(I) (7). From our gel filtration experiments we have shown that dimers are formed when Cu(II) is added to the H117G/N42C apoazurin. On the longer time scale (hours/days) a further decrease in absorption is observed because of reduction of Cu(II) to Cu(I) at the site. This phenomenon has been observed in the type 2 Cu(II)-substituted H46C and H80C Cu,Zn-superoxide dismutase mutants as well (56). However, in the case of H117G/N42C the reduction of copper is accompanied by the formation of dimers as shown by gel filtration experiments, suggesting that the metal site is still available as a sink for electrons produced during the formation of the disulfide bridge. The reduction of copper might be enhanced by the preference of the copper for a three-coordinated Cu(I) site as observed in H117G azurin (13) and similar to copper chaperones (50–55). However, the formation of an internal disulfide bond between Cys^{42} and Cys^{112} cannot be ruled out as an alternative.

Modeling—The experimental data have demonstrated that Cys^{42} plays a dominant role in binding copper and participates in the formation of a new type 2 tetragonal copper site. Although we do not want to attach too much weight to the results of the modeling studies in view of the "brute force" method used to convert the native azurin structure (Fig. 8*A*) into the structure depicted in Fig. 8*B*, the latter, with Cys^{42}, Cys^{112}, His^{46}, and Met^{121} as copper ligands, demonstrates that it is possible, indeed, to obtain a more or less strain free form of the protein that allows for binding of these four ligands to a single copper. The results once again (13, 27, 57) illustrate the increased fluxionality of the loops that make up an important part of the

hydrophobic patch, upon the introduction of the H117G mutation. There remains an uncertainty regarding the involvement of Met^{121} in copper binding. The possible involvement of water as a copper ligand, instead of Met^{121}, is under investigation.

CONCLUSION

In conclusion we have shown that the monomeric H117G/N42C azurin exhibits intriguing copper binding properties relative to wild type and H117G azurin. The double mutant uses its solvent-exposed Cys^{42} for the uptake of copper and forms a new yellow type 2 copper binding site in which Cys^{42} serves as one of the copper ligands. Resonance Raman spectroscopy provides strong evidence that the copper site is coordinated by two cysteines, which is exceptional for copper proteins. We propose a rearrangement of the loop surrounding Cys^{42}, which directs the copper toward Cys^{112} inside the protein cavity and which leads to the formation of a tetragonal copper site. His^{46} and Met^{121} are possible additional copper ligands, although their involvement is not proven.

How a living cell takes up copper from the environment and transports it to the locations inside where the metal is needed are intriguing questions that are the subjects of intensive research at the moment. It is known that transport inside the cell is often mediated by copper chaperones in which the metal, in the reduced form, is held fixed by two or three ligands, two of which consist of cysteines. The mechanism by which the metal is transferred to or from the chaperone is largely unknown. The azurin variant that has been the subject of the present study unexpectedly may constitute a model to study the mechanism of copper transfer even though the metal in this case is bound in the oxidized instead of the reduced form. The advantage of the copper being oxidized is that the metal is much more tractable, spectroscopically, than the Cu(I) form. What we have observed in the present study is that a cysteine placed on a flexible loop may quite well serve as the initial point of attachment of the copper, after which the copper may be moved by the loop to a site in the protein structure where it is temporarily stored in a more stable configuration. From there it may be mobilized for further use or transport by the reverse of this process. The data of the present study show that these processes may easily occur on the millisecond time scale.

Acknowledgments—We are grateful to T. M. Loehr and J. Ai for helpful discussions and assistance in recording resonance Raman spectra. We thank P. A. van Veelen for recording electrospray mass spectra and P. van Vliet and A. W. J. W. Tepper for help with EPR and stopped flow spectroscopy, respectively. We thank M. Swart for support with quantum mechanics/molecular mechanics calculations.

REFERENCES

1. Solomon, E. I., Baldwin, M. J., and Lowery, M. D. (1992) *Chem. Rev.* **92,** 521–542
2. Adman, E. T., and Jensen, L. H. (1981) *Isr. J. Chem.* **21,** 8–12
3. Nar, H., Messerschmidt, A., Huber, R., van de Kamp, M., and Canters, G. W. (1991) *J. Mol. Biol.* **221,** 765–772
4. den Blaauwen, T., van de Kamp, M., and Canters, G. W. (1991) *J. Am. Chem. Soc.* **113,** 5050–5052
5. den Blaauwen, T., Hoitink, C. W. G., Canters, G. W., Han, J., Loehr, T. M., and Sanders-Loehr, J. (1993) *Biochemistry* **32,** 12455–12464
6. den Blaauwen, T., and Canters, G. W. (1993) *J. Am. Chem. Soc.* **115,** 1121–1129
7. van Amsterdam, I. M. C., Ubbink, M., Jeuken, L. J. C., Verbeet, M. Ph., Einsle, O., Messerschmidt, A., and Canters, G. W. (2001) *Chem. Eur. J.* **7,** 2398–2406
8. Jeter, R. M., and Ingraham, J. L. (1984) *Arch. Microbiol.* **138,** 124–130
9. Jeuken, L. J. C., van Vliet, P., Verbeet, M. Ph., Camba, R., McEvoy, J. P., Armstrong, F. A., and Canters, G. W. (2000) *J. Am. Chem. Soc.* **122,** 12186–12194
10. Merritt, E. A., and Bacon, D. J. (1997) *Methods Enzymol.* **277,** 505–524
11. van der Spoel, D., van Buuren, A. R., Apol, E., Meulenhoff, P. J., Tieleman, D. P., Sijbers, A. L. T. M., Hess, B., Feenstra, K. F., Lindahl, E., van Drunen, R., and Berendsen, H. J. C. (1999) *GROMACS User Manual*, Bioson, Groningen, The Netherlands, www.gromacs.org
12. van Gunsteren, W. F., and Berendsen, H. J. C. (1996) *GROningen MOlecular Simulation (GROMOS) Library Manual*, Biomos, Groningen, The Netherlands, www.igc.ethz.ch/gromos/
13. Jeuken, L. J. C., Ubbink, M., Bitter, J. H., van Vliet, P., Meyer-Klaucke, W., and Canters, G. W. (2000) *J. Mol. Biol.* **299,** 737–755
14. Kroes, S. J., Salgado, J., Parigi, G., Luchinat, C., and Canters, G. W. (1996) *J. Biol. Inorg. Chem.* **1,** 551–559
15. Han, J., Loehr, T. M., Lu, Y., Valentine, J. S., Averill, B. A., and Sanders-Loehr, J. (1993) *J. Am. Chem. Soc.* **115,** 4256–4263
16. Lu, Y., Roe, J. A., Bender, C. J., Peisach, J., Banci, L., Bertini, I., Gralla, E. B., and Valentine, J. S. (1996) *Inorg. Chem.* **35,** 1692–1700
17. Mandal, S., Das, G., Singh, R., Shukla, R., and Bharadwaj, P. K. (1997) *Coord. Chem. Rev.* **160,** 191–235
18. Schnepf, R., Hörth, P., Bill, E., Wieghardt, K., Hildebrandt, P., and Haehnel, W. (2001) *J. Am. Chem. Soc.* **123,** 2186–2195
19. Andrew, C. R., Yeom, H., Valentine, J. S., Karlsson, B. G., Bonander, N., van Pouderoyen, G., Canters, G. W., Loehr, T. M., and Sanders-Loehr, J. (1994) *J. Am. Chem. Soc.* **116,** 11489–11498
20. Andrew, C. R., Han, J., den Blaauwen, T., van Pouderoyen, G., Vijgenboom, E., Canters, G. W., Loehr, T. M., and Sanders-Loehr, J. (1997) *J. Biol. Inorg. Chem.* **2,** 98–107
21. van Pouderoyen, G., Andrew, C. R., Loehr, T. M., Sanders-Loehr, J., Mazumdar, S., Hill, H. A. O., and Canters, G. W. (1996) *Biochemistry* **35,** 1397–1407
22. Liu, H., Zhu, H., Eggers, D. K., Nersissian, A. M., Faull, K. F., Goto, J. J., Ai, J., Sanders-Loehr, J., Gralla, E. B., and Valentine, J. S. (2000) *Biochemistry* **39,** 8125–8132
23. Andrew, C. R., Lappalainen, P., Saraste, M., Hay, M. T., Lu, Y., Dennison, C., Canters, G. W., Fee, J. A., Slutter, C. E., Nakamura, N., and Sanders-Loehr, J. (1995) *J. Am. Chem. Soc.* **117,** 10759–10760
24. Andrew, C. R., Fraczkiewicz, R., Czernuszewicz, R. S., Lappalainen, P., Saraste, M., and Sanders-Loehr, J. (1996) *J. Am. Chem. Soc.* **118,** 10436–10445
25. Andrew, C. R., and Sanders-Loehr, J. (1996) *Acc. Chem. Res.* **29,** 365–372
26. Alvarez, M. L., Ai, J., Zumft, W., Sanders-Loehr, J., and Dooley, D. M. (2001) *J. Am. Chem. Soc.* **123,** 576–587
27. Hammann, C., van Pouderoyen, G., Nar, H., Gomis Rüth, F.-X., Messerschmidt, A., Huber, R., den Blaauwen, T., and Canters, G. W. (1997) *J. Mol. Biol.* **266,** 357–366
28. Sandberg, A., Leckner, J., Shi, Y., Schwarz, F. P., and Karlsson, B. G. (2002) *Biochemistry* **41,** 1060–1069
29. Barrick, D. (1994) *Biochemistry* **33,** 6546–6554
30. Das, T. K., Franzen, S., Pond, A., Dawson, J. H., and Rousseau, D. L. (1999) *Inorg. Chem.* **38,** 1952–1953
31. DePilles, G. D., Decatur, S. M., Barrick, D., and Boxer, S. G. (1994) *J. Am. Chem. Soc.* **116,** 6981–6982
32. Lu, Y., Casimiro, D. R., Bren, K. L., Richards, J. H., and Gray, H. B. (1993) *Proc. Natl. Acad. Sci. U. S. A.* **90,** 11456–11459
33. McRee, D. E., Jensen, G. M., Fitzgerald, M. M., Siegel, H. A., and Goodin, D. B. (1994) *Proc. Natl. Acad. Sci. U. S. A.* **91,** 12847–12851
34. Barrick, D. (1995) *Curr. Opin. Biotechnol.* **6,** 411–418
35. Martin, A. E., Burgess, B. K., Stout, C. D., Cash, V. L., Dean, D. R., Jensen, G. M., and Stephens, P. J. (1990) *Proc. Natl. Acad. Sci. U. S. A.* **87,** 598–602
36. Maret, W., Shiemke, A. K., Wheeler, W. D., Loehr, T. M., and Sanders-Loehr, J. (1986) *J. Am. Chem. Soc.* **108,** 6351–6359
37. Czernuszewicz, R. S., LeGall, J., Moura, I., and Spiro, T. G. (1986) *Inorg. Chem.* **25,** 696–700
38. Han, S., Czernuszewicz, R. S., Kimura, T., Adams, M. W. W., and Spiro, T. G. (1989) *J. Am. Chem. Soc.* **111,** 3505–3511
39. Berlett, B. S., and Stadtman, E. R. (1997) *J. Biol. Chem.* **272,** 20313–20316
40. Cabiscol, E., Tamarit, J., and Ros, J. (2000) *Int. Microbiol.* **3,** 3–8
41. Dean, R. T., Fu, S., Stocker, R., and Davies, M. J. (1997) *Biochem. J.* **324,** 1–18
42. Konz, J. O., King, J., and Cooney, C. L. (1998) *Biotechnol. Prog.* **14,** 393–409
43. Stadtman, E. R., and Berlett, B. S. (1997) *Chem. Res. Toxicol.* **10,** 485–494
44. Valentine, J. S., Wertz, D. L., Lyons, T. J., Liou, L. L., Goto, J. J., and Gralla, E. B. (1998) *Curr. Opin. Chem. Biol.* **2,** 253–262
45. Wang, X., Ang, M. C., and Lu, Y. (1999) *J. Am. Chem. Soc.* **121,** 2947–2948
46. Blaszak, J. A., McMillin, D. R., Thornton, A. T., and Tennent, D. L. (1983) *J. Biol. Chem.* **258,** 9886–9892
47. Marks, R. H. L., and Miller, R. D. (1979) *Arch. Biochem. Biophys.* **195,** 103–111
48. Yamanaka, T., Kijimoto, S., and Okunuki, K. (1963) *J. Biochem.* **53,** 256–259
49. Nar, H., Messerschmidt, A., Huber, R., van de Kamp, M., and Canters, G. W. (1992) *FEBS Lett.* **306,** 119–124
50. Harrison, M. D., Jones, C. E., and Dameron, C. T. (1999) *J. Biol. Inorg. Chem.* **4,** 145–153
51. Harrison, M. D., Jones, C. E., Solioz, M., and Dameron, C. T. (2000) *Trends Biochem. Sci.* **25,** 29–32
52. Huffman, D. L., and O'Halloran, T. V. (2001) *Annu. Rev. Biochem.* **70,** 677–701
53. O'Halloran, T. V., and Culotta, V. C. (2000) *J. Biol. Chem.* **275,** 25057–25060
54. Rosenzweig, A. C., and O'Halloran, T. V. (2000) *Curr. Opin. Chem. Biol.* **4,** 140–147
55. Rosenzweig, A. C. (2001) *Acc. Chem. Res.* **34,** 119–128
56. Lu, Y., Gralla, E. B., Roe, J. A., and Valentine, J. S. (1992) *J. Am. Chem. Soc.* **114,** 3560–3562
57. Messerschmidt, A., Prade, L., Kroes, S. J., Sanders-Loehr, J., Huber, R., and Canters, G. W. (1998) *Proc. Natl. Acad. Sci. U. S. A.* **95,** 3443–3448
58. Jeuken, L. J. C. (2001) *The Role of the Surface-exposed and Copper-coordinating Histidine in Blue Copper Proteins*. Ph.D. thesis, pp. 129–140, University of Leiden, Leiden, The Netherlands
59. Kraulis, P. J. (1991) *J. Appl. Crystallogr.* **24,** 946–950